Full Paper Wiley Online Library ELECTROANALYSIS

DOI: 10.1002/elan.201600379

Electrode Modification Using Alkyne Manganese Phthalocyanine and Click Chemistry for Electrocatalysis

Charles. S. J. N. O'Donoghue,[a] Gertrude Fomo,[a] and Tebello Nyokong*[a]

Abstract: In this work, azidobenzene diazonium salt is grafted onto a glassy carbon electrode (GCE) followed by clicking of manganese tetrahexynyl phthalocyanine for the electrocatalysis of hydrazine. The GCE was first grafted via the in situ diazotization of a diazonium salt, rendering the GCE surface layered with azide groups. From this point, the 1,3-dipolar cycloaddition reaction, catalyzed by a copper catalyst was utilized to 'click' the manganese tetrahexynyl phthalocyanine to the surface of the grafted GCE. This new platform was then characterized using cyclic voltammetry (CV), scanning electrochemical microscopy (SECM) and X-ray photoelectron spectroscopy (XPS). Based on the cyclic voltammetry calibration curve of electrocatalysis for hydrazine, the clicked Mn phthalocyanine electrode proved to be an effective sensor with a sensitivity of 27.38 μA mM^{-1} and the limit of detection (LoD) of 15.4 pM which is a great improvement compared to other reported sensors for this analyte.

Keywords: Manganese Phthalocyanine · Electrografting · Click Chemistry · Electrocatalysis · Hydrazine

1 Introduction

Many diazonium salts have been grafted onto electrodes [1,2]. The grafting of 4- azidobenzene diazonium salt (with a terminal alkyne group) allows for the attachment of alkynyl containing complexes through "Sharpless click" reaction [3–6]. The Sharpless "click" reaction term was first used in 2001 [5]. A good example of a click chemistry reaction is the Huisgen 1,3-dipolar cycloaddition of azides and alkynes to give triazole linkages [5,6]. The reaction occurs in the presence of Cu(I) catalyst. In this work an alkynyl containing manganese phthalocyanine is used to modify a glassy carbon electrode grafted with an azide group using the click reaction.

Metallophthalocyanines (MPcs) have shown good electrocatalytic behaviour for the detection of analytes such as hydrazine, amitrole, and L-cysteine [**7**]. Manganese as a central metal for MPc, was chosen since it has various oxidation states (I–IV) which should result in favorable electrocatalytic behavior especially for reactions requiring multi-electron transfer. In addition, MnPc derivatives have shown improved electrocatalytic oxidation of hydrazine [**7**], which is used as a test analyte in this work. Hydrazine is heavily used in chemical industry, and has been implicated as a carcinogen and is readily absorbed through the skin [8].

Alkynyl substituted MPc complexes are known [9–13], and the synthesis of Mn tetrakis(5-hexyn-oxy) phthalocyanine (complex **1**, Scheme 1) employed in this work has been reported [13]. However, apart from our recent report on alkynyl substituted FePc [14,15], there are no reports on electrode modification using click chemistry and alkynyl Pcs. This is the first time that an alkynyl MnPc is employed. The combination of grafting and click chemistry offers a covalent attachment of MPcs onto the electrode, resulting in a stable layer, hence it is employed in this work. The modified electrodes are characterized by various techniques including X-ray photoelectron spectroscopy, scanning electrochemical microscopy, and various electrochemical methods.

2 Experimental

2.1 Materials

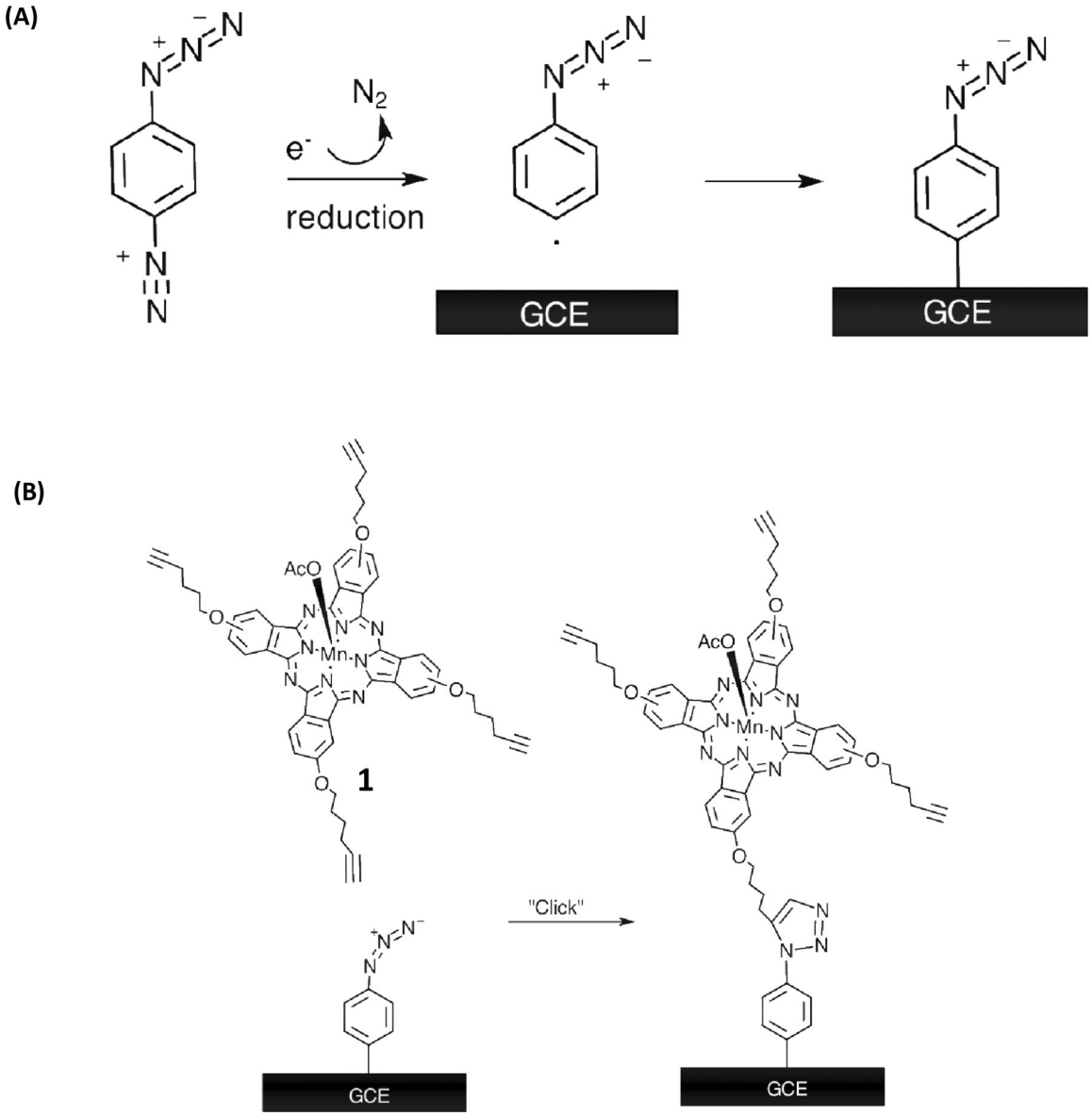
Millipore water was obtained from Milli-Q Water Systems (Millipore Corp. Bedford, MA, USA). Alumina (≤ 10 μm), dimethylformide (DMF), dimethyl sulfoxide (DMSO), copper(I)complex ($Cu(PPh_3)_3Br$), tetrabutyl ammonium tetrafluoroborate ($TBABF_4$), trimethylamine and hydrazine monohydrate were purchased from Sigma Aldrich and used as they are received. Acetonitrile (ACN) was obtained from Minima. Iron ferricyanide and iron ferrocyanide were obtained from Unilab and used as received. Dichloromethane (DCM) was obtained from B&M Scientific. 4-Azidobenzenediazonium salt was synthesized as reported in literature [16].

2.2 Equipment

An Autolab PGSTAT30 electrochemical workstation (equipped with GPES software version 4.9) was used for cyclic voltammetry (CV), chronoamperometry and electrochemical impedance spectroscopy (EIS). Scanning electrochemical microscopy (SECM) experiments were conducted using Uniscan equipment, model 370 and

[a] C. S. J. N. O'Donoghue, G. Fomo, T. Nyokong
Department of Chemistry, Rhodes University, Grahamstown 6140, South Africa
Tel: +27 46 6038260; Fax: +27 46 6225109;
*e-mail: t.nyokong@ru.ac.za

 © 2016 Wiley-VCH Verlag GmbH & Co. KGaA, Weinheim



Scheme 1. Presentation of (A) the grafting of diazonium salt to the GCE and (B) clicking of (OAc)Mn tetrakis(5-hexyn-oxy) phthalocyanine (complex **1**) to the grafted electrode. OAc = acetate.

a 25 μm Pt ultra-microelectrode (UME) as the tip. Approach curve analysis and constant height imaging were employed. The 25 μm Pt micro-electrode was used together with a Pt counter electrode and Ag|AgCl wire as the pseudo-reference electrode. Changes in the steady state current of $K_3[Fe(CN)_6]$ oxidation at 0.29 V vs. Ag|AgCl were monitored. X-ray photoelectron spectroscopy (XPS) was done using a Kratos Axis Ultra DLD, with the Al (monochromatic) anode, equipped with a charge neutraliser. For wide XPS scans, the following parameters were used: emission 10 mA, anode (HT): 15 kV, operating pressure below 5×10^{-9} Torr, hybrid lens, and resolution to acquire scans was at 160 eV pass energy in slot mode. The centre used for the scans was at 520 eV and the width at 1205 eV, with steps at 1 eV and dwell time at 100 ms. For the high resolution scans, the resolution was changed to 40 eV pass energy in slot mode. Centre was at 402 eV and width at 12 eV for N(1s), with step size at 0.05 eV and dwell time at 500 ms. Glassy carbon plates (1 cm × 1 cm and 2 mm thick) were obtained from Goodfellow, UK and employed for SECM and XPS studies.

2.3 Electrochemical Methods

A three electrode electrochemical cell comprising of a glassy carbon electrode (GCE) (geometric area = 0.071 cm^2) as the working electrode, Ag|AgCl (3 M KCl) as reference electrode, and a platinum wire as the counter electrode was employed. The GCE surfaces were polished on a Buehler-felt pad using alumina (0.05 μm). The glassy carbon plate (GCP) (used for SECM and XPS) was power cleaned using 3 μm diamond paste, followed

 © 2016 Wiley-VCH Verlag GmbH & Co. KGaA, Weinheim

by 0.25 μm diamond paste and then polished on a Buehler-felt pad using alumina (0.05 μm). For all electrodes, following the polishing step, sonication was carried out for 5 min in Millipore water to remove any impurities. The surfaces were then rinsed with Millipore water and dried in an oven at 60 °C under nitrogen.

The bare GCE surface was grafted (Scheme 1A) by electrodeposition and scanning from +0.5 V to −1 V for 5 cycles in a solution of 0.1 mM 4-azidobenzenediazonium tetrafluoroborate (containing 0.01 M $TBABF_4$ in 96 : 4 CANACN : HCl (1 M)) following reported methods [17–20]. Between each step of grafting, the electrode was rinsed thoroughly via ultrasoncication for 5 min with milli-Q water, to give grafted-GCE. Following the grafting step, the click reaction (Scheme 1B) was performed by immersing the grafted electrode into a solution containing 0.1 μM complex **1** in 5 mL DMF containing 2 mM $Cu(PPh_3)_3Br$ and 2 ml triethylamine. The electrode was left to 'click' with complex **1** for 18 h, represented as **1**-clicked-GCE. The glassy carbon plate (GCP) surfaces used for SECM and XPS were grafted and 'clicked' via the same process as applied to the GCE, represented as grafted-GCP and **1**-clicked-GCP.

3 Results and Discussion

3.1 Characterization of Modified Electrode

3.1.1. Cyclic Voltammetry (CV)

Electrode modification through grafting is well known [17–20]. In this work, the GCE was first grafted using a diazonium salt, which forms a radical by losing an electron and releasing a nitrile. The resulting radical on the benzene ring forms a covalent bond with the GCE surface, Scheme 1A. CV confirmed that the grafting step was successful, the characteristic reduction peak was seen and consequently disappeared with subsequent scans. The GCE surface was then further modified by the click reaction with complex **1** (to form **1**-clicked-GCE, Scheme 1B). It is possible for multiple arms of complex **1** to 'click' to the azide groups. This may generate flatter patches of surface and may cause 'hollows' to form. It is also possible that complex **1** could have aggregated and thereby 'clicked' multiple complexes to one site and generate a large bump. CVs of the modified electrode, post 'clicking', in $K_3[Fe(CN)_6]$ solution show the blocking effect, as CV curves appear as straight lines in comparison to the reversible couple observed on the bare electrode (figure not shown).

3.1.2. Scanning Electrochemical Microscopy (SECM)

The area scan technique of SECM was employed to assess the uniformity of the modified surface. The bare surface was first scanned to generate data for comparison (Fig. 1A). The bare GCP had an average current of 1.08×10^{-8} A. The bare GCP also showed that it was not completely smooth, based on the surface plot produced. Some hollows and bumps were present. The grafted-GCP surface produced a 3 dimensional surface plot that showed what would appear to be an inconsistently modified surface (Fig. 1B). However, the grafted-GCP surface shows a mainly uniform surface, hence suitable for application in clicking complex **1** to the surface. The grafted-GCP surface showed a current range of 1.02 to 1.14×10^{-8} A, unlike the more uniform current of 1.08×10^{-8} A at the bare GCP.

The **1**-clicked-GCP surface scan (Fig. 1C) shows similar results to those obtained for the grafted-GCP surface. Bumps and undulations were observed. **1**-clicked-GCP surface showed larger bumps compared to grafted-GCP surface. This could be due to complex **1** being a larger molecule with several orientations on the surface following the click reaction. The passivation effect was also seen in the area scan as the average current is lower for **1**-clicked-GCP surface (the order of 10^{-9} A, Fig. 1C (b and c)), compared to the grafted-GCP or bare-GCP surfaces with the order of 10^{-8} A, Fig. 1B and Fig. 1C(a). By examining different areas of the electrode surface following clicking with complex **1**, scans produced showed that the unmodified area (Fig. 1C(a)) exhibits more conductivity than areas that are grafted-GCP and **1**-clicked-GCP, Fig. 1C (b) and (c). The protrusions in Fig. 1C(b) could be due to parts of the electrode that are not modified since they have higher currents.

3.1.3. X-ray Photoelectron Spectroscopy

Fig. 2A shows the high resolution spectra of the N(1s) region for the grafted-GCP (a) and **1**-clicked-GCP (b). Following grafting, Fig. 2A(a), the peaks at 398.1 and 403.6 eV are characteristic of azide groups on the surface. Following clicking, the peak at 403.6 eV is now absent Fig. 2A(b). These changes are representative of the formation of the 1,2,3-triazole, confirming successful 'clicking'. A general change in nitrogen intensity is observed following clicking (Fig 2C), which confirms the success of the click reaction.

In the C 1s spectra (Fig. 2B), the grafted-GCP surface (Fig. 2B (a)) exhibits a peak at 286.6 eV, which could be associated with the carbon to azide group bonding. The 286.6 eV peak is absent in the **1**-clicked-GCP surface (Fig. 2B(b)) suggesting the click reaction has taken place, as the quantity of azides have reduced heavily. Secondly, there is a peak at 283.2 eV in the **1**-clicked-GCP spectra (Fig. 2B(b)) that was not present in the grafted-GCP spectra, which could be attributed to a carbon oxygen single bond from the attached MnPc.

3.2. Electrocatalytic Behavior towards Hydrazine

3.2.1 Cyclic Voltammetry

Fig. 3 shows the effect of the clicked MnPc on the surface of the electrode for sensing the hydrazine. The CVs were scanned in a window of −1 V to 1 V vs. Ag|AgCl in a solution of 0.2 M NaOH. In Fig. 3 the CVs for electrooxida-

 © 2016 Wiley-VCH Verlag GmbH & Co. KGaA, Weinheim

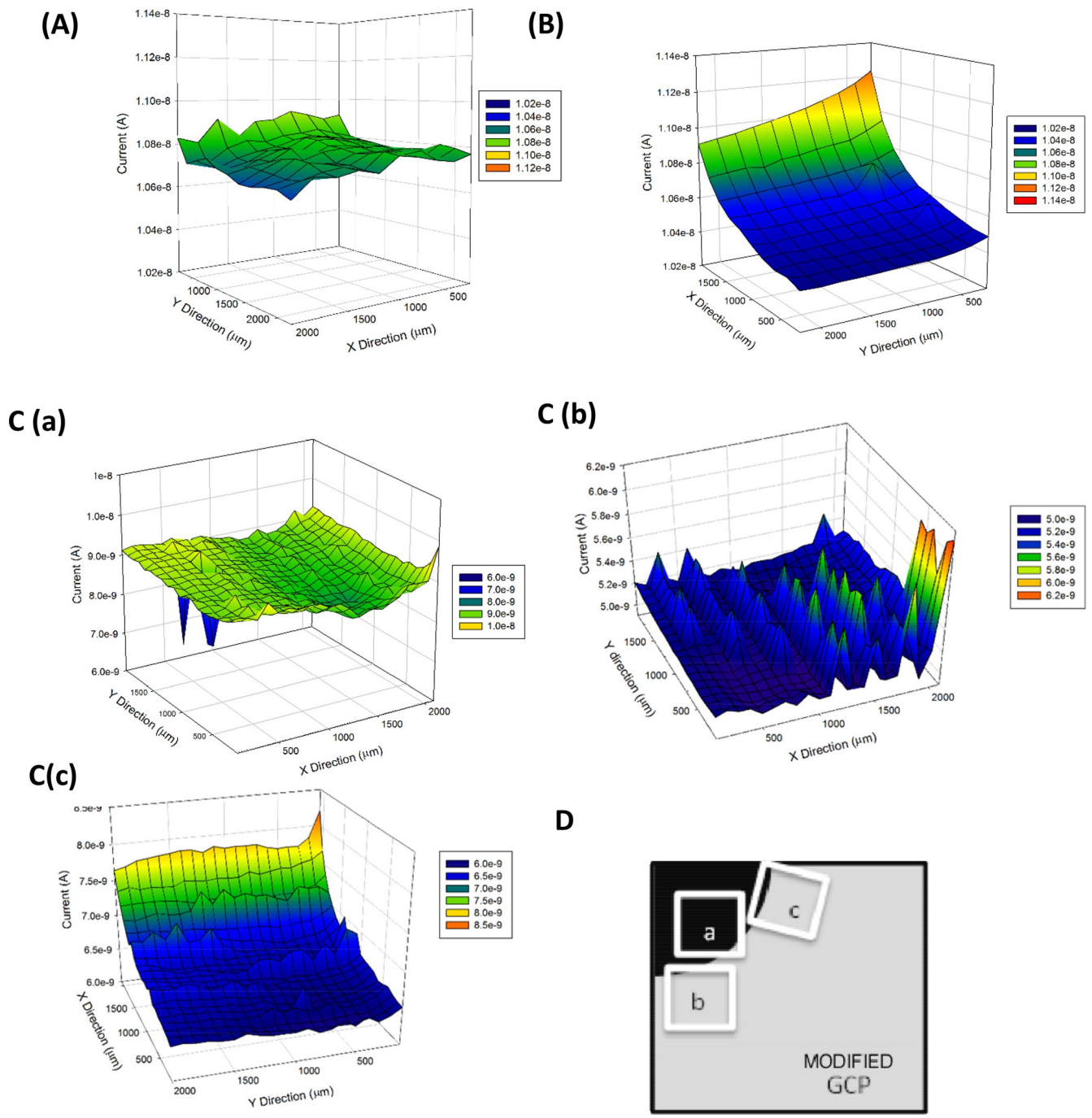


Fig. 1. SECM Micrograph on (A) bare-GCP, (B) grafted-GCP and (C) **1**-clicked-GCP surface. For C, (a), (b) and (c) refer to D. (a) represents the unmodified section.

tion of hydrazine on **1**-clicked-GCP, grafted-GCE and bare GCE are compared. The latter two do not show a clear hydrazine oxidation peak. In contrast, **1**-clicked-GCP exhibited a clear oxidation peak at 0.34 V. This potential is however, more positive than reported for clicked FePc at +0.1 V [13] and −0.1 V [21].

The mechanism for hydrazine oxidation on MnPc complexes has been reported [22] and is as follows (equations 1 to 3, axial acetate ligand left out for simplicity):

$$Mn(III)Pc + N_2H_4 \rightarrow [Mn(II)Pc]^- \ldots (N_2H_4)^+] \quad (1)$$

$$[Mn(II)Pc]^-(N_2H_4)^+ + OH^- \rightarrow Mn(III)Pc\ldots N_2H_3 + H_2O + e^- \quad (2)$$

$$Mn(III)Pc\ldots N_2H_3 + OH^- \rightarrow H_2O + Mn(III)Pc + N_2H_2 + e^- \quad (3)$$

 © 2016 Wiley-VCH Verlag GmbH & Co. KGaA, Weinheim

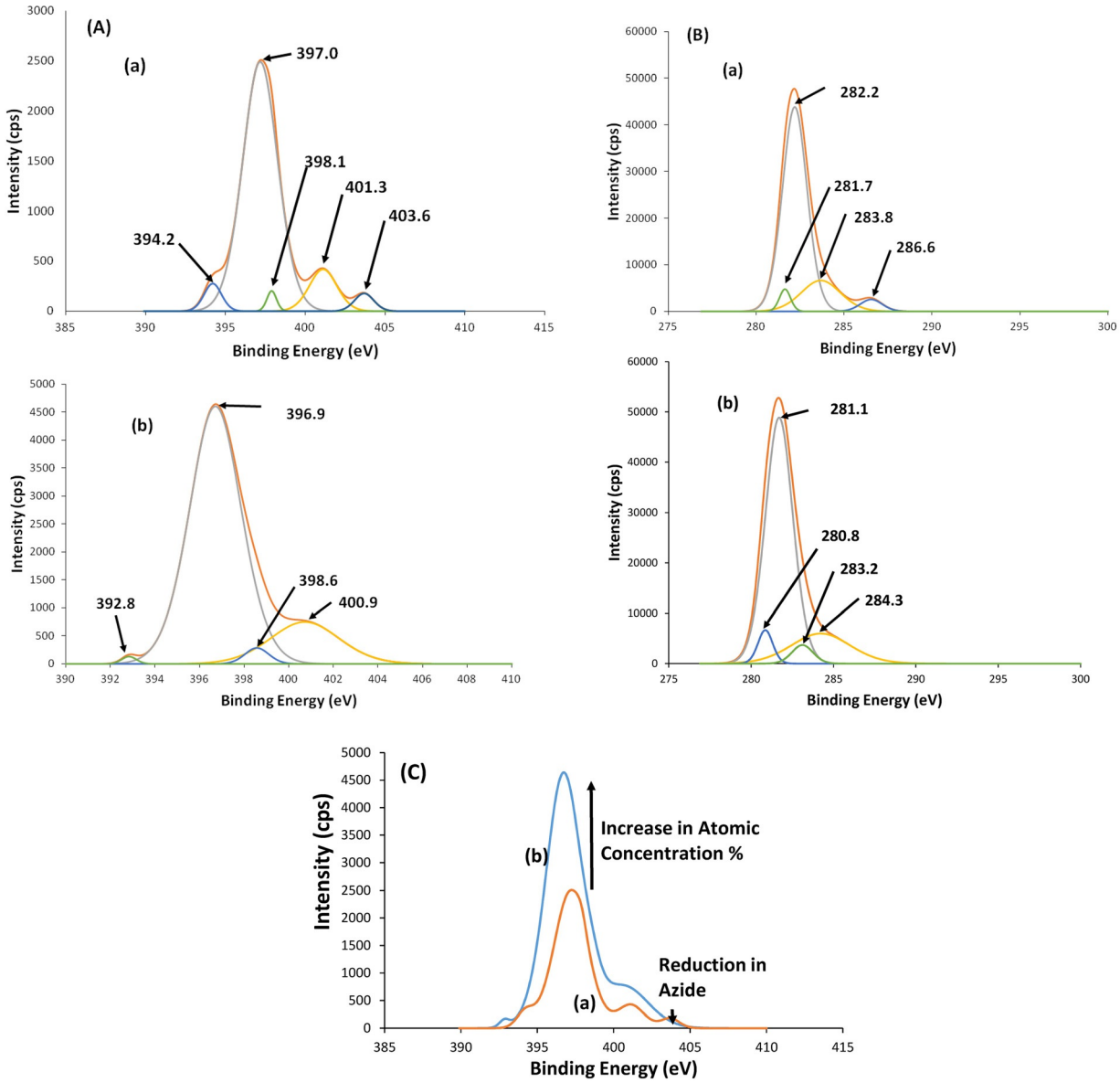


Fig. 2. High resolution XPS spectra for (A) N1s and (B) C1s for (a) grafted-GCP and (b) **1**-clicked-GCP. (C) shows the comparison of the curve fitted envelope for N1s for (a) grafted-GCP and (b) **1**-clicked-GCP.

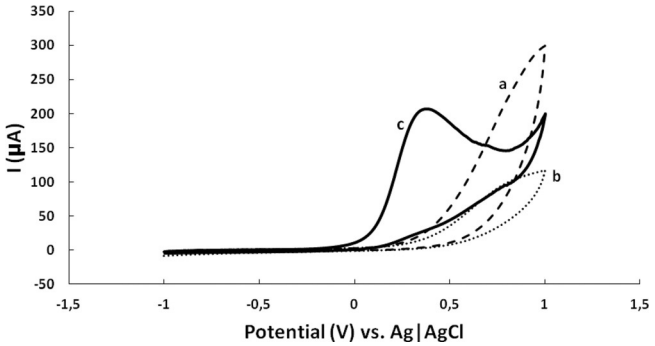


Fig. 3. Cyclic voltammograms for (a) bare GCE, (b) grafted-GCE and (c) **1**-clicked-GCE in 0.2 M NaOH containing 6 mM of hydrazine.

Fig. 4A shows the CVs obtained when the scan rate was varied. Fig. 4B and C show linear plots of current against square root of scan rate and peak potential vs. the log of scan rate, respectively. The linearity of the plot in Fig. 4B confirms that the catalytic oxidation of hydrazine is diffusion controlled. The relationship between peak potential and log scan rate for an irreversible diffusion-controlled process is given by Equation (4) [23].

$$E_p = \frac{2.3RT}{2(1-\alpha)n_\alpha F}\log v + K \qquad (4)$$

where α is the transfer coefficient, n_α is the number of electrons involved in the rate determining step, v is the

 © 2016 Wiley-VCH Verlag GmbH & Co. KGaA, Weinheim

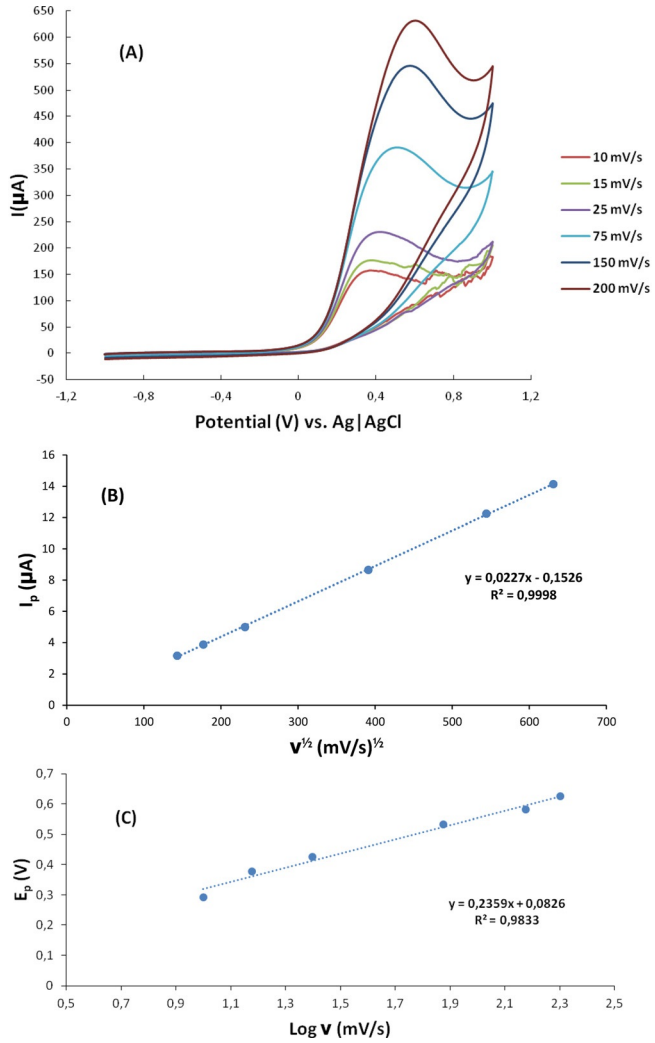


Fig. 4. (A) CVs of **1**-clicked-GCE at different scan rates. Plots of (B) current (I/μA) vs. square root scan rate (v/mV/s) and (C) peak potential (E/V) vs. log (v/mV/s) vs. Ag|AgCl, in 6 mM hydrazine in 0.2 M NaOH.

scan rate, K is a constant, R is the universal gas constant and T is the temperature. The plot of E_p vs. log v (Fig. 4C) produced a linear relationship and the Tafel slope was calculated to be 471.8 mV decade^{-1}, by multiplying the slope of E_p vs. log v by 2, Equation (5):

$$E_p = \frac{b}{2}\log v + K \quad (5)$$

High Tafel slope values above the normal 60–120 mV decade^{-1} have no kinetic meaning and are related to electrochemical steps [24] or to substrate-catalyst interactions in a reaction intermediate [25–27].

The stability of modified metal surface as a new platform is of primary interest, particularly in electrochemical sensor. This stability depends on the conducting composite materials and the method used to modify the electrode surface. The stability of **1**-clicked-GCE towards the detection of hydrazine was investigated by recording consecutive CV scans of hydrazine (6 mM in 0.2 M NaOH) (Fig. 5). The **1**-clicked-GCE electrode can be considered as stable as there is little fluctuation with the repetitive scanning, only a slight decrease in intensity.

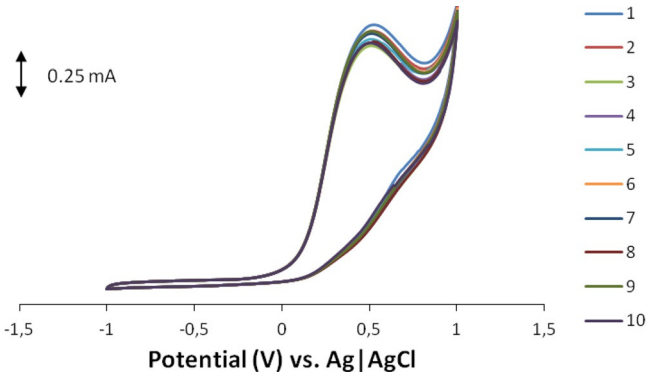


Fig. 5. Repetitive scans (10) with **1**-clicked-GCE in 0.2 M NaOH with 6 mM hydrazine.

The insert in Fig. 6 shows a linear relationship between hydrazine concentration and current from 0 to 2 mM (generated from the CVs in Fig. 6). Based on the calibration curve, the limit of detection (LoD) was determined using the 3δ/slope ratio notation where δ is the standard deviation of 10 plots of sensor in NaOH. The value of the detection limit was calculated to be 15.4 pM with the correlation constant of $R^2 = 0.993$. The estimated sensitivity of the sensor was 27.38 μA mM^{-1}. The limit of detection for the sensor was relatively low compared to the one reported by Ozoemena (in order of the micromolar range [28]) using Co(II)P and Nxele *et al.* (1.09 μM) using Fe(II)P [14]. The toxicity limit for hydrazine is said to be 3 μM [8] and the LoD for this work is 15.4 pM, therefore the sensor is capable of detecting at much lower levels, enabling a more sensitive detection. The sensor developed in this work could also be useful for the agricultural industry, where hydrazine is used as a pesticide, in addition to applications in the chemical industry.

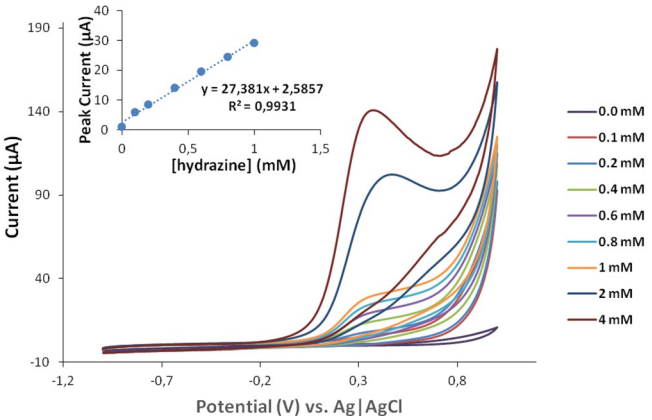


Fig. 6. CVs of **1**-clicked-GCE in 0.2 M NaOH variable concentrations of hydrazine. Insert: plot of peak current (μA) vs. concentration of hydrazine.

 © 2016 Wiley-VCH Verlag GmbH & Co. KGaA, Weinheim

3.2.2. Electrochemical Impedance Spectroscopy

The Nyquist plot ($Z_{imaginary}$ vs. Z_{real}) (Fig. 7A) is divided into two frequency regions, the kinetically controlled (high frequency) region where the semi-circle is observed and the diffusion controlled (low frequency) region where the Warburg line is observed. The diameter of the semi-circle gives the charge transfer resistance (R_{CT}). A high R_{CT} signifies low conductivity of the electrodes. The characteristic semicircles exhibited are most pronounced for the bare than the grafted-GCE and **1**-clicked-GCE at high frequencies. For the bare, the grafted-GCE and **1**-clicked-GCE, the R_{ct} values were estimated to be 6701 Ω, 5395 Ω and 999 Ω respectively. This shows that the R_{ct} value after click chemistry is approximately six times smaller than that of the bare GCE, which indicates that the Mn(III)Pc facilitates the electron transfer process, thus corroborating the CVs of Fig. 3. The apparent electron transfer rate constant (k_{app}) was obtained from equation 6 [28]:

$$K_{app} = RT/F^2 R_{ct} C \quad (6)$$

where C is the concentration of the hydrazine (in $mol\,L^{-1}$). The calculated k_{app} values for **1**-clicked-GCE ($4.44\times10^{-8}\,cm\,s^{-1}$), grafted-GCE ($8.22\times10^{-9}\,cm\,s^{-1}$) and the bare-GCE ($6.61\times10^{-9}\,cm\,s^{-1}$) are of different magnitude. The high k_{app} value for the **1**-clicked-GCE is indicative of faster electron transfer process compared to the bare GCE. From the charge transfer resistance, the exchange current density and interfacial heterogeneous standard rate transfer constant can be calculated using the Equations 7 and 8 [29]:

$$R_{ct} = \frac{RT}{dF_{i_0}} \leftrightarrow i_0 = \frac{RT}{nFR_{ct}} \quad (7)$$

$$i_0 = nFAk^0C^* \leftrightarrow k^0 = \frac{i_0}{nFAC^*} \quad (8)$$

where n is the number of electrons transferred, i_0 is the standard exchange current (A), A is the geometric area of the electrode (cm^2), k^0 is the heterogeneous standard rate transfer constant ($cm\,s^{-1}$), C* is the concentration of hydrazine. The calculated values of i_0 are 1.76×10^{-6} A, 4.76×10^{-6} A and 2.57×10^{-5} A for bare-GCE, grafted-GCE and **1**-clicked-GCE respectively, and the k^0 values were determined to be 1.28×10^{-9}, 3.47×10^{-9} and $1.87\times10^{-8}\,cm\,s^{-1}$ for bare-GCE, grafted-GCE and **1**-clicked-GCE, respectively. The i_0 and k^0 values using **1**-clicked-GCE are very high compared to those obtained using grafted-GCE and bare-GCE. This shows that the rate of oxidation of hydrazine is faster when using the modified **1**-clicked-GCE, hence the importance of Mn(III)Pc as catalyst in the electrocatalysis process of hydrazine.

Fig. 7B shows the Bode plot characteristic change of phase angle θ against the logarithms of frequency response of the system. From the Bode plots (Fig. 7B), the bare GCE showed symmetrical peak with a maximum value of 76° at 184 Hz corresponding to the relaxation process of the GCE|solution interface. Modification of the GCE led to the changes in θ values (64° at 91 Hz for **1**-clicked-GCE). The reduction of the phase angle and frequency indicates that the catalytic reaction takes place at the surface of the Mn(III)Pc film but not on the bare and the grafted-GCE.

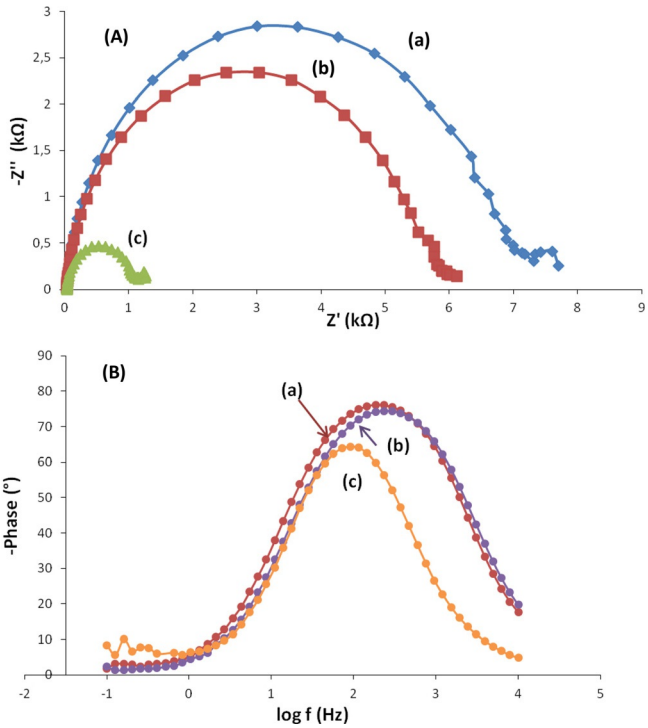


Fig. 7. Nyquist (A) and Bode plots for (a) bare GCE, (b) grafted GCE and (c) **1**-clicked-GCE recorded in 0.2 M NaOH containing 6 mM of hydrazine.

3.2.3. Chronoamperometry

Fig. 8A shows the response of the clicked GCE towards different concentrations of hydrazine. From the plot of peak current vs. concentration of hydrazine (Fig. 8A, insert, $R^2=0.997$) the sensitivity of the electrode of $7.33\,\mu A\,mM^{-1}$ and LoD of 34.8 pM were obtained which are less favourable than those obtained by CV at $27.38\,\mu A\,mM^{-1}$ and 15.4 pM, respectively, discussed above. CV performed better than chronoamprometry in terms of evaluating sensitivity and LoD, for these studies.

The catalytic current (I_{cat}) is dominated by the rate at which hydrazine is oxidized on the modified surface of the GCE. The slopes of the plots of (I_{cat}/I_{buff}) vs. $t^{1/2}$ (Fig. 8B) were used to determine the rate constant according to Equation (9) [30].

$$\frac{I_{cat}}{I_{buff}} = \gamma^{\frac{1}{2}}\pi^{\frac{1}{2}} = \pi^{\frac{1}{2}}(k_{cat}Ct)^{\frac{1}{2}} \quad (9)$$

 © 2016 Wiley-VCH Verlag GmbH & Co. KGaA, Weinheim

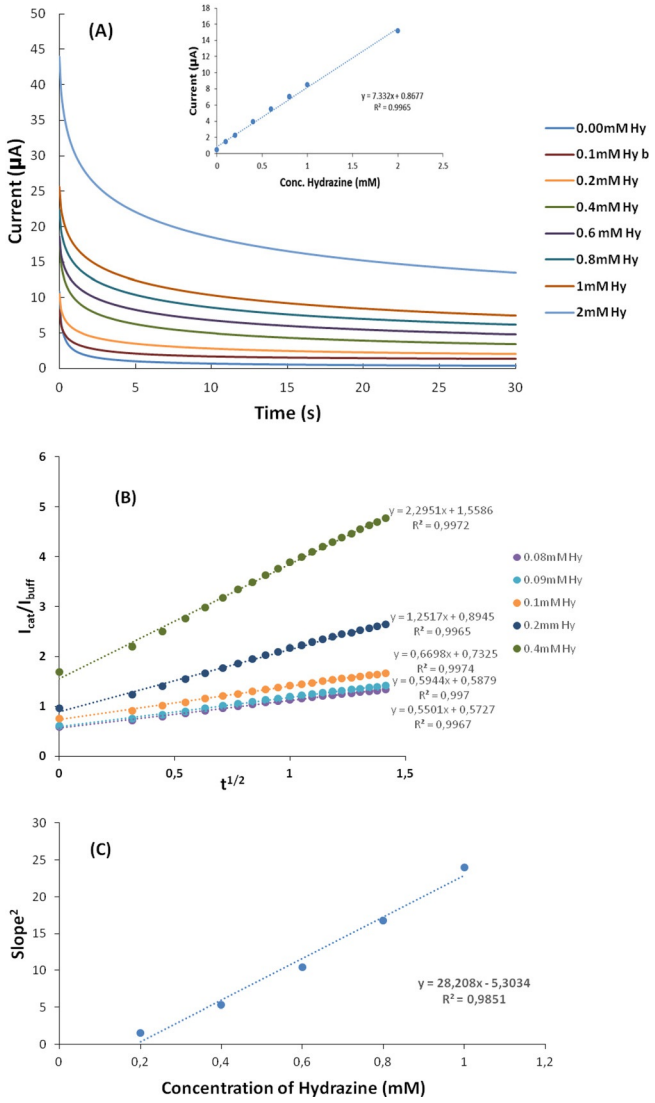


Fig. 8. (A) Chronoamperometric response to hydrazine in 0.2 M NaOH at various concentrations, insert = plot of peak current (µA) vs. concentration of hydrazine. (B) plot of (I_{cat}/I_{buff}) vs. $t^{1/2}$ and (C) plot of the squares of the slopes from B.

where I_{cat} represents the current when the analyte is present, I_{buff} represents current in the NaOH alone without analyte, k_{cat} is the catalytic constant, C is the concentration of hydrazine and t is the time in elapsed seconds. By plotting the square of the slopes obtained from Fig. 8B vs. the concentration of hydrazine, a linear relationship can be observed, Fig. 8C and is represented by Equation (10).

$$y = 29.766[hydrazine]\left(\frac{s^{-1}}{mM}\right) - 6.512s^{-1}, R^2 = 0.9924 \quad (10)$$

The slope of this plot is equivalent to πk. The value of k_{cat} was calculated as $4.1\times10^3\ M^{-1}s^{-1}$. This value is within the range of k_{cat} values $\sim10^3\ M^{-1}s^{-1}$ reported for the detection of hydrazine on phthalocyanine-modified electrodes [28,31]. This result is an improvement on work previously reported [14].

4 Conclusions

Glassy carbon electrode surfaces were successfully modified via the click reaction between an azide (grafted on a glassy carbon electrode) and a terminal alkynyl group of a Mn phthalocyanine. The electrode was characterized with SECM and XPS as well as electrochemical analysis. The modified surfaces also successfully catalyzed hydrazine. The electrode could be an efficient and robust sensor for hydrazine as it had a sensitivity of 27.38 µA mM^{-1} and a LoD of 15.4 pM from cyclic voltammetry studies. This sensor shows its true strength in its stability, as it can be left untouched for weeks and still detect hydrazine in the same way it would do after recent preparation.

Acknowledgements

This work was supported by the Department of Science and Technology (DST) and National Research Foundation (NRF), South Africa through DST/NRF South African Research Chairs Initiative for Professor of Medicinal Chemistry and Nanotechnology (UID 62620) as well as Rhodes University and DST/Mintek Nanotechnology Innovation Centre (NIC) – Sensors, South Africa.

References

[1] D. Bélanger, J. Pinson, *Chem. Soc. Rev.* **2011**, *40*, 3995.
[2] A. J. Gross, C. Bucher, L. Coche-Guerente, P. Labbé, A. Downard, J.-C. Moutet, *Electrochem.Commun.* **2011**, *13*, 1236.
[3] V. V. Rostovtsev, L. G. Green, V. V. Fokin, K. B. Sharpless, *Angew. Chem. Int. Ed.* **2002**, *41*, 2596.
[4] D. Evrard, F. Lambert, C. Policar, V. Balland, B. Limoges, *Chem. Euro. J.* **2008**, *14*, 9286.
[5] H. C. Kolb, M. G. Finn, K. B. Sharpless, *Angew. Chem. Int. Ed.* **2001**, *40*, 2004.
[6] Z. P. Demko, K. B. Sharpless, *Angew. Chem. Int. Ed.* **2002**, *41*, 2113.
[7] T. Nyokong, Electrodes Modified with Monomeric M-N4 Catalysts for of Environmentally Important Molecules, in: J. H. Zagal, F. Bedioui, J.-P. Dodelet (Eds.), N4-Macrocyclic Metal Complexes, Springer, USA **2006**, 315.
[8] G. Choudhary, H. Hansen, *Chemosphere* **1998**, *37*, 801.
[9] Y. Yilmaz, M. K. Şener, I. Erden, U. Avciata, *Polyhedron.* **2009**, *28*, 3419.
[10] A. Kalkan, A. Koca, Z. A. Bayir, *Polyhedron* **2004**, *23*, 3155.
[11] C. C. Leznoff, Z. Li, H. Isago, A. M. D'Ascanio, D. S. Terekhov, *J. Porphyrins Phthalocyanines.* **1999**, *3*, 406.
[12] N. Cauchon, H. Tian, R. Langlois, C. Madeleine, S. Martin, H. Ali, D. Hunting, D. J. E. van Lier, *Photochem. Photobiol. Sci.* **2010**, *9*, 331.
[13] D. Quinton, E. Antunes, S. Griveau, T. Nyokong, F. Bedioui, *Inorg. Chem.Commun.* **2011**, *14*, 330.
[14] S. R. Nxele, P. Mashazi, T. Nyokong, *Electroanalysis* **2015**, *27*, 2468.

 © 2016 Wiley-VCH Verlag GmbH & Co. KGaA, Weinheim

[15] S. R. Nxele, T. Nyokong, *Electrochim. Acta* **2016**, *194*, 26.
[16] D. Evrard, F. Lambert, C. Policar, V. Balland, B. Limoges, *Chem.: Euro. J.* **2008**, *14*, 9286.
[17] D. Bélanger, J. Pinson, *Chem. Soc. Rev.* **2011**, *40*, 3995.
[18] J. C. Lacroix, G. Trippe-Allard, J. Ghilane, P. Martin, *Adv. Nat. Sci.: Nanosci. Nanotechnol.* **2014**, *5*, 015001 (6pp).
[19] M. Delamar, R. Hitmi, J. Pinson, J. M. Saveant, *J. Am. Chem. Soc.* **1992**, *114*, 5883.
[20] F. Matemadombo, P. Westbroek, T. Nyokong, *Electrochim. Acta* **2007**, *53*, 480.
[21] M. Coates, T. Nyokong, *J. Electroanal. Chem.* **2012**, *687*, 111.
[22] J. H. Zagal, S. Lira, S. Ureta-Zañartu, *J. Electroanal. Chem.* **1986**, *210*, 95.
[23] A. Bard, L. Faulkner, in Electrochemical Methods: Fundamentals and Applications, Wiley, New York **2006**.
[24] C. A. Caro, F. Bedioui, J. H. Zagal, *Electrochim. Acta* **2002**, *47*, 1489.
[25] B. Wemeckes, F. Beck, *Electrochim. Acta* **1985**, *3.0*, 1491.
[26] M. E. G. Lyons, C. A. Fitzgerald, M. R. Smyth, *Anal.* **1994**, *119*, 855.
[27] J. M. Zen, A. S. Kumar, M. R. Chang, *Electrochim. Acta* **2000**, *45*, 1691.
[28] K. I. Ozoemena, *Sensors* **2006**, *6*, 874.
[29] P. M. O. R. A. Ndangili, S. N. Mailu, R. F. Ngece, A. Jijana, A. Williams, F. Iftikhar, P. G. L. Baker, I. E. Iwuoha, *Int. J. Electrochem. Sci.* **2011**, *6*, 1438.
[30] C. X. Guo, F. Hu, X. Lou, C. Li, *J. Power Sources* **2010**, *195*, 4090.
[31] M. M. Ardakani, M. A. Karimi, M. M. Zare, S. M. Mirdehghan, *Int. J.Electrochem. Sci.* **2008**, *3*, 246.

Received: June 7, 2016
Accepted: June 21, 2016
Published online: July 21, 2016

 © 2016 Wiley-VCH Verlag GmbH & Co. KGaA, Weinheim